A comparative statistical analysis of equivalent linear and nonlinear site response in the Kathmandu Valley, Nepal

D. Poudyal[1,2], N. Nordin[1] and S.N.A. Roslan[3]

[1] Department of Civil Engineering, Infrastructure University Kuala Lumpur, Kajang, Selangor Darul Ehsan, Malaysia
[2] Department of Civil Engineering, Nepal Engineering College, Changunarayn, Bhaktapur, Nepal
[3] Department of Civil Engineering, Universiti Putra Malaysia, Serdang, Salangar, Malaysia

ABSTRACT   This study presents a comparative assessment of equivalent linear (EL) and nonlinear (NL) site response analyses for the Kathmandu Valley, Nepal, using DEEPSOIL™ based on borehole data from multiple locations and seismic input motions focusing on two significant events: the Gorkha (M_w 7.8, 25 April 2015) and Kobe, Japan (M_w 6.9, 17 January 1995) earthquakes. A statistical analysis, including Pearson correlation, normality tests, t-tests, and Mann-Whitney U tests, was conducted using MATLAB to examine the relationship between peak ground acceleration (*PGA*) and displacement under EL and NL conditions. Results show that the NL analysis better captures soil nonlinearity. The Gorkha NL case showed a strong inverse correlation (slope = −20.195, *p* = 0), indicating significant displacement reduction with increasing *PGA*. EL cases, in contrast, exhibited weaker trends, often overestimating. Boxplots further confirmed significant differences in *PGA* and displacement between events, especially under EL conditions. These findings highlight the critical importance of incorporating NL site response analysis in seismic hazard assessments. The Gorkha NL results reveal that NL models can reduce predicted displacement by more than 50% compared to EL models. This has direct implications for infrastructure resilience in earthquake-prone regions like the Kathmandu Valley, where site-specific NL analysis is essential for accurate seismic design and safety evaluation.

Key words: displacement, equivalent linear analysis, nonlinear analysis, *PGA*, statistical test.

1. Introduction

Site response analysis, a critical component of seismic hazard evaluation, examines how local soil conditions modify ground motion during an earthquake. Two primary approaches are used: equivalent linear (EL) and nonlinear (NL) analysis. EL methods assume constant soil properties for each strain compatible cycle, making them computationally efficient, but less accurate under strong shaking. In contrast, NL analysis considers changes in soil stiffness and damping with strain, allowing for more realistic simulation of soil behaviour during intense seismic events. These methods are vital for predicting ground motion characteristics, guiding the design of earthquake resilient infrastructure, and improving seismic microzonation efforts.

Nepal, located at the tectonic boundary between the Indian and Eurasian plates, is one of the most seismically active regions in the world (Poudyal *et al.*, 2025a). The Kathmandu Valley,

encompassing the districts of Kathmandu, Lalitpur, and Bhaktapur (Fig. 1), is the largest urban centre of Nepal, with a population of approximately 2.9 million (National Planning Commission, 2022). The unique geological setting and rapid urbanisation of the valley make it highly susceptible to seismic hazards (Poudyal *et al.*, 2025b), and displacement is a key parameter that reflects the extent of ground movement during seismic events (Delaviz *et al.*, 2024). It is directly linked to structural damage, foundation instability, and ground deformation, making it crucial for assessing seismic hazards and designing earthquake resilient infrastructure. Particularly in regions like the Kathmandu Valley, where soft soils amplify seismic waves, understanding displacement patterns is essential for accurate hazard assessments and effective mitigation strategies. The 2015 Gorkha Nepal earthquake (M_w 7.8, 25 April 2015), along with its aftershock at Dolkha District (M_w 7.3, 12 May 2015), were among the most devastating seismic events in the history of Nepal, causing widespread damage across districts such as Sindhupalchowk, Kathmandu, Nuwakot, and Bhaktapur (Poudyal *et al.*, 2022). Similarly, on 3 November 2023, a 6.4-magnitude earthquake struck the Jajarkot district in Nepal, with its epicentre in Ramidanda (Fig. 1). This earthquake resulted in 157 fatalities, including 105 in Jajarkot and 52 in Rukum West, and caused injuries to hundreds more. The tremors were felt as far as Kathmandu, Delhi, and several districts in Bihar, India, highlighting the widespread impact of seismic activity in the region.

Ground response analysis has been widely applied to assess seismic risks in various geologic contexts (Mishra *et al.*, 2025). Globally comparative studies such as those by Edincliler and Tuncay
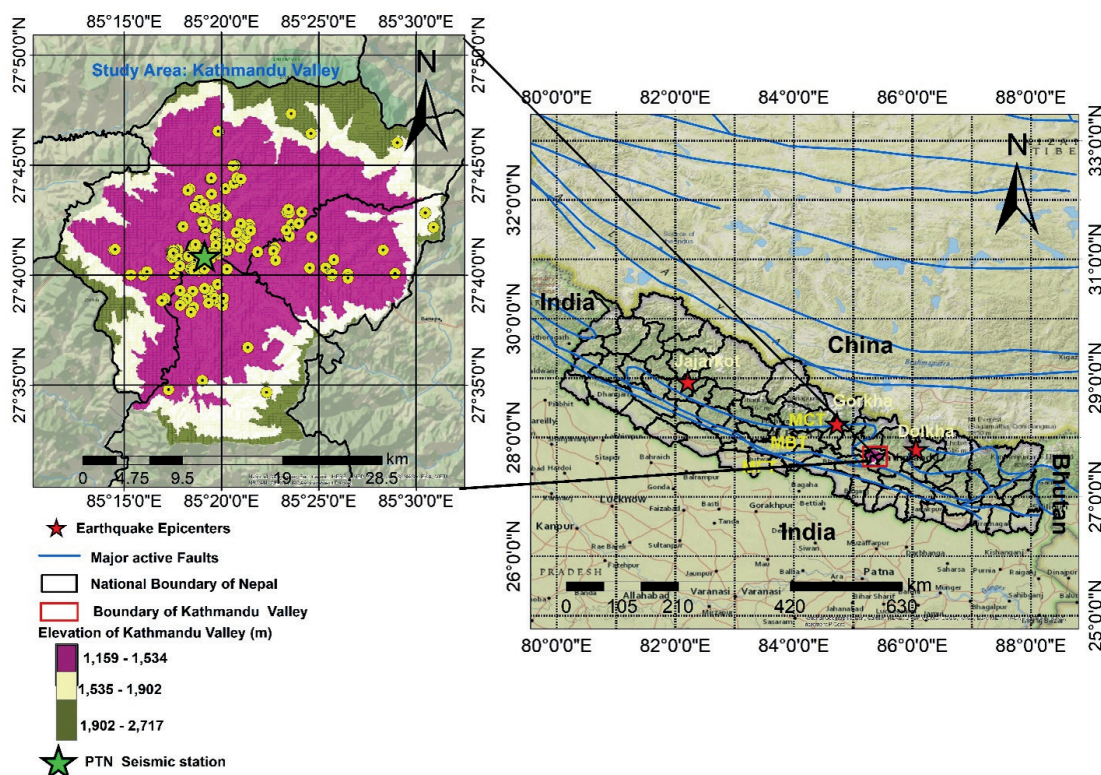

Fig. 1 - Left: the study area, Kathmandu Valley, with elevation zoning, borehole locations, and labelled districts. Right: regional tectonic setting of Nepal showing major faults, earthquake epicentres (Gorkha earthquake: M_w 7.8, 25 April 2015; Dolkha earthquake: M_w 7.3, 12 May 2015; and Jajarkot earthquake: M_w 6.4, 3 November 2023), and neighbouring countries India, China, and Bhutan. The red rectangle indicates the location and spatial extent of the Kathmandu Valley shown in the main map.

(2018) used DEEPSOIL™ to compare EL and NL site response analyses for Bodrum city, Turkey, under two earthquake motions, the Bodrum/Kos and Gokçeada earthquakes. For the Gokçeada event, peak ground acceleration (*PGA*) reductions of 69% and 68% were observed using EL, while NL analysis showed larger reductions of 122% and 305% for the same boreholes. Similarly, under the Bodrum/Kos earthquake, EL analysis resulted in *PGA* reductions of 56% and 33% and NL analysis showed reductions of 192% and 294%, respectively. Xiao *et al.* (2022) analysed rock and soft soil sites in China using DEEPSOIL™ software. Their findings indicated that the EL method was more effective in capturing strong NL behaviour in rock sites during intense seismic events, whereas the NL method revealed a notable weakening effect in soft soils. Despite both site types being deemed safe, soft soil sites demonstrated relatively better seismic performance. Mahmood *et al.* (2020) studied a site in Peshawar, Pakistan, using both EL and NL approaches to evaluate parameters such as mobilised shear strength, shear strain, and ground acceleration. Their analysis showed similar amplification factors (~2.4) at the fundamental period, although the EL method produced slightly higher *PGA* values.

While Tran *et al.* (2021) examined cultural heritage sites in Hanoi, Vietnam, employing one-dimensional (1D) EL and NL site response analyses to study seismic wave propagation, they reported that the EL method resulted in a higher surface *PGA* (0.2 g) compared to the NL method (0.16 g). Khan and Waseem (2019) performed a site response analysis at two active seismic regions in Pakistan (Shakardarra and Muzaffarabad) using EL and NL methods under vertical ground motions of 7.0 M_l and 4.9 m_b using nonlinear earthquake response analysis (NERA) and equivalent-linear earthquake response analysis (EERA). Despite high stress levels, the soils showed negligible strains. At Shakardarra, EL analysis yielded *PGA* values up to 0.38 g, while NL values were lower (e.g. 0.35 g for sandy gravel). At Muzaffarabad, EL results were as high as 0.83 g, with significantly reduced values in the NL analysis (0.21 g for sandy gravel).

Yildiz (2021) in Istanbul, Turkey, has compared EL and NL site response analysis using DEEPSOIL™ to evaluate soil behaviour under the 1999 Kocaeli earthquake motion. Modelled soil profiles were analysed for spectral acceleration, *PGA*, and lateral displacement. EL tends to overestimate *PGA* due to its simplified linear assumptions, whereas NL more accurately reflects NL soil behaviour by incorporating strain-dependent stiffness and damping. Despite its limitations, EL remains popular due to its simplicity, but the findings emphasise the importance of using NL for more realistic seismic site response predictions, especially in layered soil profiles.

In Nepal, research on ground response analysis considering statistical tests remains limited. While Chamlagain and Gautam (2015) use the 1991 Uttarkashi earthquake (M_w 6.8, 20 October, Uttarakhand, northern India) to conduct the EL site response analyses using EERA software, Gautam *et al.* (2017) analysed deep borehole logs and presented results on amplification factor and ground acceleration using NL ground response analysis considering the Uttarkashi earthquake as the input motion. Pagliaroli *et al.* (2018) conducted 1D and two-dimensional site response analyses in the Kathmandu Valley, emphasising the impact of mainshock and aftershock recordings on seismic response, guiding the development of seismic risk mitigation strategies while Poudyal (2019) conducted linear site response analysis using SHAKE software which resulted in surface acceleration values for 14 boreholes of the Kathmandu Valley and reported a soil amplification factor of 1.6. Likewise, Guragain *et al.* (2020) used DEEPSOIL™ software and the EL approach to conduct a 1D ground response analysis on the ground motion caused by the Kobe earthquake of Japan (M_w 6.9, 17 January 1995). Using both linear and NL approaches, Bhusal *et al.* (2022) assessed the seismic response in softer soil recorded for Dharahara (also known as the Bhimsen Tower and a historical landmark located in central Kathmandu) and lithologies in Kathmandu using DEEPSOIL™ software. Similarly, Poudyal (2024, 2025c) used DEEPSOIL™

software to conduct a 1D NL response analysis in the Kathmandu Valley, considering the Gorkha earthquake as input motion to calculate the *PGA*, soil amplification, and soil vulnerability index.

This study offers a novel and comprehensive comparison between EL and NL ground response analyses, utilising DEEPSOIL™ software for simulating seismic loading in the Kathmandu Valley. By examining two significant seismic events, the Gorkha (2015) and Kobe (1995) earthquakes, this study addresses the limitations of traditional site response analysis methods. The use of both EL and NL methods enables a deeper understanding of the dynamic behaviour of soil under different seismic intensities, with particular emphasis on the NL effects that better capture soil hysteretic behaviour and energy dissipation mechanisms, which are crucial during high intensity events.

A unique aspect of this study is the incorporation of local borehole data from the Kathmandu Valley, including soil types, shear wave velocity, and unit weight, ensuring that the analysis accurately reflects the geological characteristics of the region. This is a significant departure from previous studies that rely on generic datasets, providing more site-specific insights. Furthermore, by comparing the NL and EL models, the study shows that NL methods lead to a stronger reduction in displacement with increasing *PGA*, particularly for the Gorkha earthquake, highlighting the critical role of NL soil behaviour in moderating seismic response.

This study also distinguishes itself by employing a robust statistical framework, including Pearson correlation analysis, normality tests, t-tests, and Mann-Whitney U tests, to evaluate the relationship between *PGA* and displacement across the two earthquakes. These analyses provide statistical rigor in comparing the two seismic events, while regression models help to visually capture the trend in seismic response. Additionally, this study adopts an advanced bedrock definition, modelling it as a rigid half space, which improves the accuracy of soil structure interaction simulations and reflects the latest advancements in site response analysis. By focusing on the Kathmandu Valley and combining both linear and NL approaches, this study offers new insights into seismic hazard assessment and infrastructure resilience, crucial for earthquake-prone regions. These findings underscore the importance of considering NL effects in seismic modelling, as traditional elastic models may underestimate displacement and overestimate structural stability during strong earthquakes. Thus, the findings of this study are pivotal for improving seismic hazard evaluations and enhancing infrastructure resilience in the Kathmandu Valley.

2. Seismicity of Nepal

The Himalayas, a notable example of tectonic formation, emerged from the collision between the Tibetan and Indian plates. Three basic thrusts, the Main Frontal Thrust (MFT), Main Boundary Thrust (MBT), and Main Central Thrust (MCT), as depicted in Fig. 1, are shaped by the seismic attributes of the faults moving from north to south. The MFT is often visualised as fragmented thrusts emerging from the Main Himalayan Thrust (MHT), where the Indian tectonic plate subducts beneath the Eurasian plate. Among the thrust systems, the MBT currently demonstrates the highest activity, while the MCT has remained active for centuries. Conversely, the MFT is perceived as the most recent thrust system. Moving south from the MBT, the Lesser Himalayas are constituted by sedimentary layers. Further south, the Outer Himalayas consist of sedimentary deposits of the Miocene epoch, which display bending and fracturing along the Earth's crust. This extensive mountain range spans across Bhutan, China, India, Nepal, and Pakistan. For the Kathmandu Valley, site specific seismotectonic investigations highlight the direct influence of

these active faults. While the MCT has demonstrated long-term seismic activity across centuries, the proximity of the valley to the MBT and MFT makes it particularly susceptible to strong ground shaking. Historical earthquakes such as the 1934 Bihar Nepal (M_w 8.1) and the 2015 Gorkha (M_w 7.8) events underscore the seismic threat of the valley. Proximity to both the MFT and MBT makes the valley highly susceptible to strong ground shaking, emphasising the need to incorporate local geological and geotechnical conditions into seismic hazard assessments.

3. Data and methodology

3.1. Ground response analysis

Response analysis is the process of determining the propagation of shear waves induced by seismic loading within boreholes (Amjadi and Johari, 2022). This process quantifies how soil deposits impact the motion of waves as they propagate through the ground. Such analysis can be executed by different methods, such as the linear, EL, and NL methods (Kramer, 1996). For this analysis, two different methodologies were used: a) the EL method and b) the NL method.

The EL model is a very popular approach for representing soil nonlinearity. In order to estimate the real NL and inelastic behaviour of soil, Schnabel et al. (1972) introduced an EL approach. This method uses shear modulus and damping ratio values to represent the linear behaviour of soil. By iteratively updating these values, the EL model accounts for the inelastic behaviour of the soil, improving the accuracy of the analysis (Iswanto and Yee, 2016). In contrast, the NL method more explicitly captures the hysteretic behaviour of the soil by modelling the dynamic response in the time domain. The workflow for comparing both analyses is outlined in Fig. 2.

Seismic loading can induce pore water pressure, which reduces soil stiffness and alters its behaviour (Zhang et al., 2023). The EL approach may not fully capture these effects, particularly
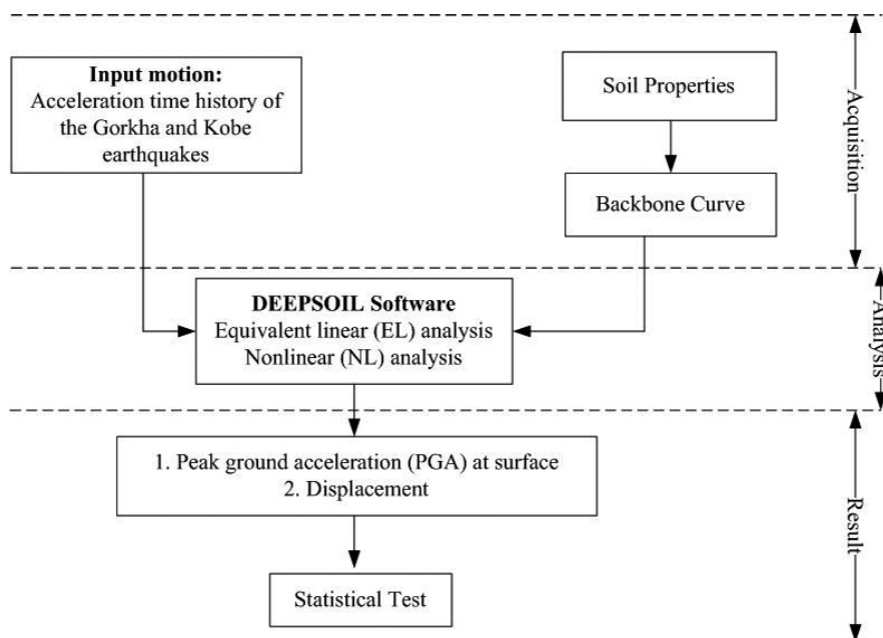

Fig. 2 - Methodological illustration for the comparison of the two analyses

when significant soil nonlinearity is present. To address this, NL ground response analysis provides a more accurate representation of soil behaviour under seismic loading. In this study, DEEPSOIL™ software was selected for the analysis as it is capable of conducting both frequency- and time-domain seismic response analyses. The software uses a pressure-dependent hyperbolic model, which is well suited for representing soil nonlinearity, particularly in soft soil regions like the Kathmandu Valley.

3.2. Borehole data

This study uses 225 borehole data from various locations within the Kathmandu Valley, as shown in Fig. 1, and its three-dimensional (3D) visualisation of boreholes, as shown in Fig. 3. The lithological data includes a range of soil types, such as dense to extremely dense soils, moderately dense soils, sands, gravels, and silts. Key parameters such as soil thickness, standard penetration test (SPT), N-value shear wave velocity, and soil unit weight are used in both the linear and NL analyses. The depth of the water table was taken from available lithology data. For boreholes without explicit water table information, it was assumed to be at ground surface. All the geotechnical information, including soil stratigraphy, SPT N-value shear wave velocity, unit weight, and water table depth, are detailed in the supplementary material.
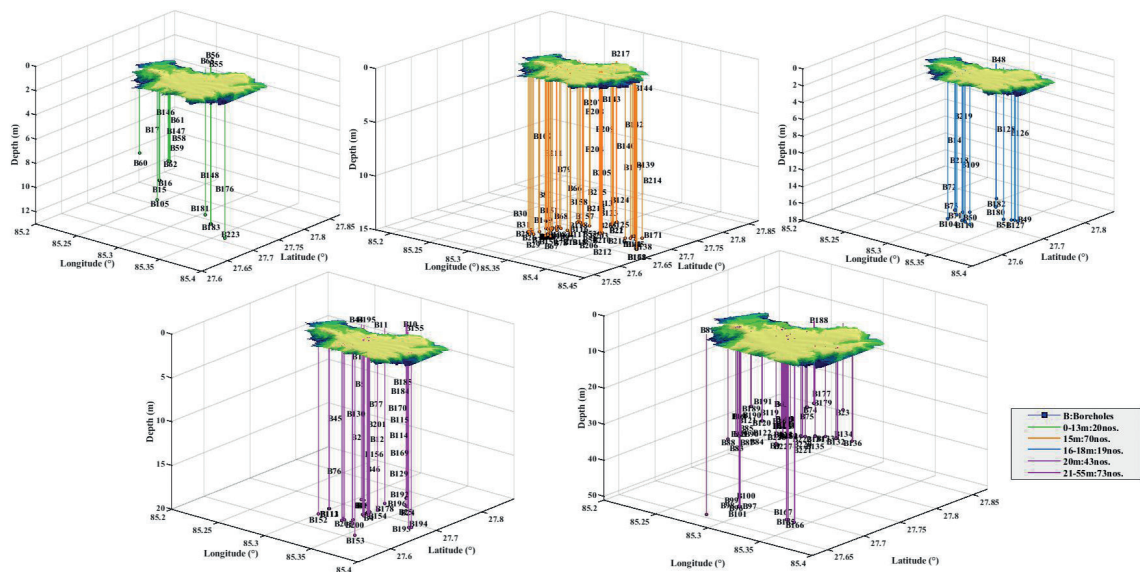

Fig. 3 - 3D visualisation of borehole locations across the study area and in five different depth ranges, illustrating spatial distribution and depth variation.

3.3. Wave propagation

In this study, a 1D vertical wave propagation scheme was adopted. Here, seismic shear waves are assumed to propagate upwards, through horizontally layered soil deposits, from the bedrock to the ground surface. This approach is commonly used for site response analysis in deep alluvial basins such as the Kathmandu Valley, where horizontal stratification dominates. The soil profile

at each borehole location was idealised as a series of layers defined by thickness, shear wave velocity, unit weight, and damping characteristics. Within this framework, the EL and NL analyses differ primarily in how soil nonlinearity is incorporated during wave propagation. The EL method applies an iterative process in the frequency domain, updating shear modulus and damping ratio until convergence is achieved at an effective strain level. The NL method, on the other hand, directly integrates the equations of motion in the time domain, capturing strain dependent hysteresis and modulus degradation throughout the propagation path. By modelling how the input bedrock motion is modified as it travels through the soft sediments of the valley, the wave propagation scheme enables the quantification of amplification effects, frequency shifts, and energy dissipation. This provides the foundation for a comparative evaluation between EL and NL approaches in the Kathmandu Valley.

3.4. The equivalent linear method

The EL method is widely used in site response analysis to approximate NL soil behaviour (Dicleli and Buddaram, 2007). It estimates shear modulus (G) and damping ratio (ξ) at a specific shear strain level using an iterative process. This method is computationally efficient and provides reasonable accuracy in capturing soil nonlinearity under seismic loading (Wang *et al.*, 2023). In the EL approach, the shear modulus and damping ratio are functions of the effective shear strain (γ_{eff}), typically expressed as:

$$G = G_{max}*f_G\left(\gamma_{eff}\right) \tag{1}$$

$$\xi = f_\xi\left(\gamma_{eff}\right) \tag{2}$$

where, G_{max} is the maximum (small-strain) shear modulus, $f_G(\gamma_{eff})$ and $f_\xi(\gamma_{eff})$ are the modulus reduction and damping ratio curves, respectively.

The iteration in the EL method begins with an initial assumption of γ_{eff}. Based on this value, the corresponding G and ξ are obtained from the modulus reduction and damping curves. These parameters are, then, used to perform a site response analysis, which produces an updated value of γ_{eff}. This updated strain is compared with the previously assumed value and, if they differ, the process is repeated. The iteration continues until the input and output γ_{eff} levels converge, indicating consistency and compatibility among G, ξ, and γ_{eff}. Equivalent response analysis is conducted using a maximum frequency which refers to the highest frequency that a particular layer can propagate. Very dense soil layers in a soil column attenuate high frequency components of earthquake waves, resulting in an underestimation of site response at these higher frequencies. The thickness of every soil layer is calculated using Eq. (3), which considers the maximum frequency (f_{max}) that the soil can transmit.

$$f_{max} = \frac{V_s}{4H}. \tag{3}$$

To address this issue, Hashash *et al.* (2020) recommended modelling thick soil layers as thinner layers with a thickness, H, that allows the propagation of frequencies up to at least 30 Hz. This approach ensures that high frequency ground motions are accurately captured, providing a proper response at high frequencies (Groholski *et al.*, 2016).

For the upper 30-metre soil column, Eq. (4) established by Saifuddin *et al.* (2021) is used in this study. For all soil types:

$$V_S = 115.8N^{0.251} \tag{4}$$

where V_s is the shear wave velocity, N is the average blow counts of the SPT per layer.

3.5. The nonlinear method

In NL time domain analysis, dynamic motion Eq. (5) is solved incrementally using numerical methods. During each time step, the hysteretic performance of the soil is modelled, and the stiffness and damping matrices are updated accordingly (Hashash *et al.*, 2020)

$$m\ddot{u} + c\dot{u} + k\dot{u} = -m\ddot{u}_g \tag{5}$$

where m is the mass matrix, c is the damping matrix, k is the stiffness matrix, u is the displacement vector, $\dot{u}$ and $\ddot{u}$ are the velocity and acceleration vectors, $\ddot{u}_g$ is the ground acceleration vector.

The soil column is divided into discrete strata using either finite elements or a multi degree of freedom lumped parameter model (Kramer, 1996). Each layer is modelled by a mass, a dashpot for viscous damping, and a NL spring in numerous time domain solutions. Half of the mass of the two adjacent layers at their common boundary is combined to generate the mass matrix. In this study, the soil modulus reduction and damping curves (Figs. 4a and 4b) were developed using the pressure-dependent modified Kondner Zelesko - (MKZ) approach introduced by Darendeli (2001), as illustrated in Fig. 4.

This model accounts for the strain dependent degradation of shear modulus and the increase in damping with strain under cyclic loading. The MKZ formulation incorporates the effect of

This model accounts for the strain dependent degradation of shear modulus and the increase
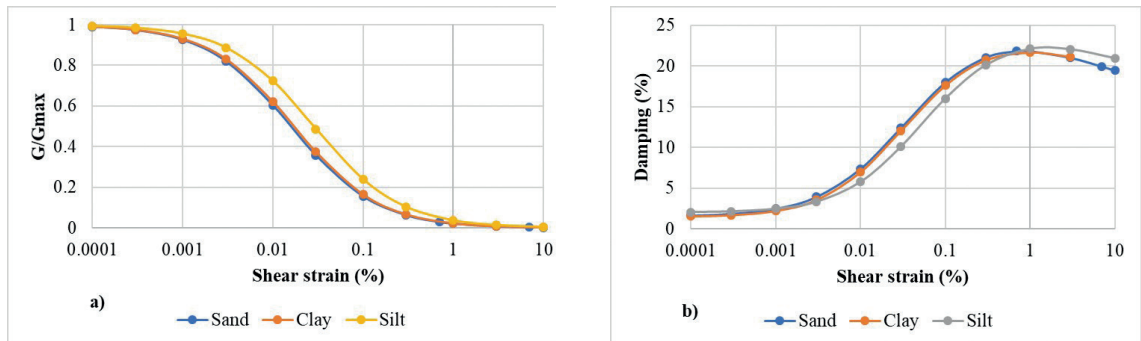

Fig. 4 - Dynamic properties of the soil: a) G/G_{max} modulus reduction curve b) damping curve with respect to shear strain.

in damping with strain under cyclic loading. The MKZ formulation incorporates the effect of confining pressure on soil stiffness, enabling more realistic simulation of soil response under seismic excitation. For hysteretic behaviour, the non Masing reloading/unloading rule was

employed to capture nonlinearity beyond the classical Masing rules. This method considers factors such as confining pressure, plasticity index (*PI*), friction angle (*ϕ*), over consolidation ratio (*OCR*), excitation frequency (*f*), and number of loading cycles (*N*). Based on the soil data available for the study area, *PI* values ranging from 3.2% to 36% and *ϕ* values between 17° and 38° were adopted. For generating the reference dynamic curves within the Darendeli model, the coefficient of Earth pressure at rest (K_o) was determined from Hashash *et al.* (2020), while the *OCR*, *N*, and *f* parameters were set to 1, 10, and 1, respectively, throughout the analysis.

3.6. Input ground motion

The networks of Hokkaido University in Japan and Tribhuvan University in Nepal were active prior to the earthquake that struck Gorkha. Its four stations are located at the Central Department of Geology at the Tribhuvan University, Pulchowk Campus (PTN) at the Institute of Engineering Lalitpur, Thimi Bhaktapur at the University Grants Commission and at a rock site in Kirtipur (Takai *et al.,* 2016). In this study, the input motion of the Kobe and the Gorkha earthquakes, as depicted in Fig. 5, are employed as input ground motion to enable DEEPSOIL™ to simulate seismic loading. The Gorkha earthquake was recorded at the PTN station (27.6815° N - 85.31896° E; Fig. 1), while the Kobe earthquake was recorded at the close Takatori station in Japan (34.59° N - 135.04° E; Fig. 6). For the N-S, E-W, and vertical components, the highest horizontal accelerations were 0.15g, 0.13 g, and 0.15 g at the PTN station for the Gorkha earthquake and 0.83 g, 0.58 g, and 0.34 g at the Takatori station for the Kobe earthquake, respectively.
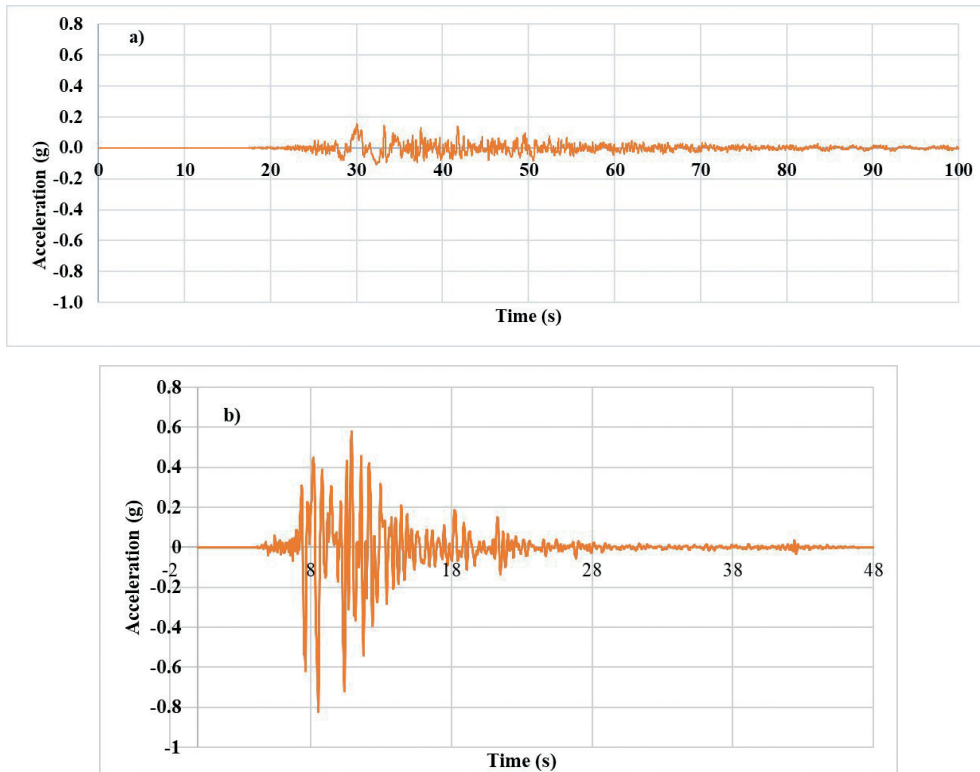

Fig. 5 - Input motion: a) the Gorkha earthquake recorded by the PTN station located at Pulchowk Campus, Lalitpur, b) the Kobe earthquake recorded by the Takatori station, Japan.

Fig. 6 - Kobe earthquake showing the earthquake epicentre (34.59° N, 135.04° E) and the Takatori seismic station (34.65° N, 135.14° E)

3.7. Bedrock definition

Pandey and Jakka (2022) investigated the impact of bedrock/half space depth and found that seismic bedrock (V_s ~ 760 m/s) may not be appropriate for most geological conditions. Falcone *et al.* (2020) also observed that the dense soil layer (V_s ~ 760 m/s) should not be classified as bedrock, as deeper layers and impedance significantly influence site response. Although the significance of stiffness and bedrock in site response analysis is widely acknowledged, there are currently no clear guidelines for selecting these parameters. Therefore, in this study, bedrock is characterised as a rigid half space to account for the limitations identified by previous research. This approach ensured a more precise assessment of surface spectral acceleration, accounting for the effects of stiffness and damping resulting from soil structure interaction. To accurately replicate the dynamic response of the system and solve the NL equations of motion [Eq. (5)], integration techniques were employed. The variation of values between *PGA* versus depth and displacement versus depth, illustrated in the Section Results and discussion, shows the comparison between EL and NL.

3.8. Statistical analysis

The study begins with data acquisition and preprocessing, where *PGA* and displacement values recorded during the Gorkha and Kobe earthquakes under EL and NL conditions, are imported into MATLAB. Once the data is loaded, a Pearson correlation analysis is conducted to evaluate the relationship between *PGA* and displacement. This correlation (*r*) is quantified using the Pearson correlation coefficient [Eq. (6)], along with the statistical significance (*p*-value), to determine whether a strong linear relationship exists between the parameters:

$$r = \frac{\sum (X_i - X^-)(Y_i - Y^-)}{\sqrt{(X_i - X^-)^2} * \sqrt{(Y_i - Y^-)^2}}$$

(6)

where X_i and Y_i represent the *PGA* and displacement values, respectively, $\overline{X}$ and $\overline{Y}$ are their mean values. Following the correlation analysis, statistical comparisons are performed to assess differences between the earthquake datasets. First, normality tests using the Kolmogorov-Smirnov test determine whether the data follow a normal distribution. If the data are normally distributed, a two-sample t-test is applied to compare means between the Gorkha and Kobe earthquakes. If non-normality is detected, the Mann-Whitney U test is used as a non-parametric alternative to assess significant differences. The results help establish whether EL and NL conditions significantly affect seismic responses. To further explore the relationship between *PGA* and displacement, scatter plots are generated. A least-squares regression line is fitted to the data using the polynomial fitting function, providing a visual representation of trends in the seismic response. This regression analysis helps identify how *PGA* and displacement interact under different conditions. Finally, a comparative boxplot analysis is conducted to visualise the distribution and spread of *PGA* and displacement values under EL and NL conditions for both earthquakes. Boxplots highlight median values, interquartile ranges, and the presence of outliers, offering insights into variability and differences in seismic response. These combined analyses provide a comprehensive understanding of how EL and NL conditions influence *PGA* and displacement across different seismic events.

Although DEEPSOIL™ generates response spectra, this study focused on *PGA* as the principal intensity measure to map spatial variability. *PGA* was selected due to its direct relevance for seismic hazard mapping on basin scale. A more detailed period-dependent spectral acceleration analysis, while important for structural design applications, is recommended for future work.

4. Results and discussion

In this study, a comparison between EL and NL ground response analysis was conducted using DEEPSOIL™ software. The comparison is made between two input motions and their statistical tests using MATLAB. The analysis of the results focuses on the relationship between *PGA* and displacement for two earthquake events, Gorkha (2015) and Kobe (1995), under both EL and NL conditions.

4.1. Peak ground acceleration distribution

The spatial distribution of *PGA* for EL and NL analyses, presented in Fig. 7, is based on DEEPSOIL™ simulations for the 2015 Gorkha and 1995 Kobe earthquake motions. In the EL case, relatively higher *PGA* values are observed in the northern and central parts of the Kathmandu Valley, whereas Lalitpur and the southern region of Bhaktapur show comparatively lower values. Under the NL condition, *PGA* values decrease across much of the basin, with a more pronounced reduction in areas underlain by deep sedimentary deposits. This pattern is consistent with the damping and stiffness degradation effects associated with NL soil response. A comparison between the two earthquakes indicates that the Kobe input motion generates higher *PGA* values than the Gorkha motion for both the EL and NL cases, primarily due to stronger input motion characteristics and local site conditions.
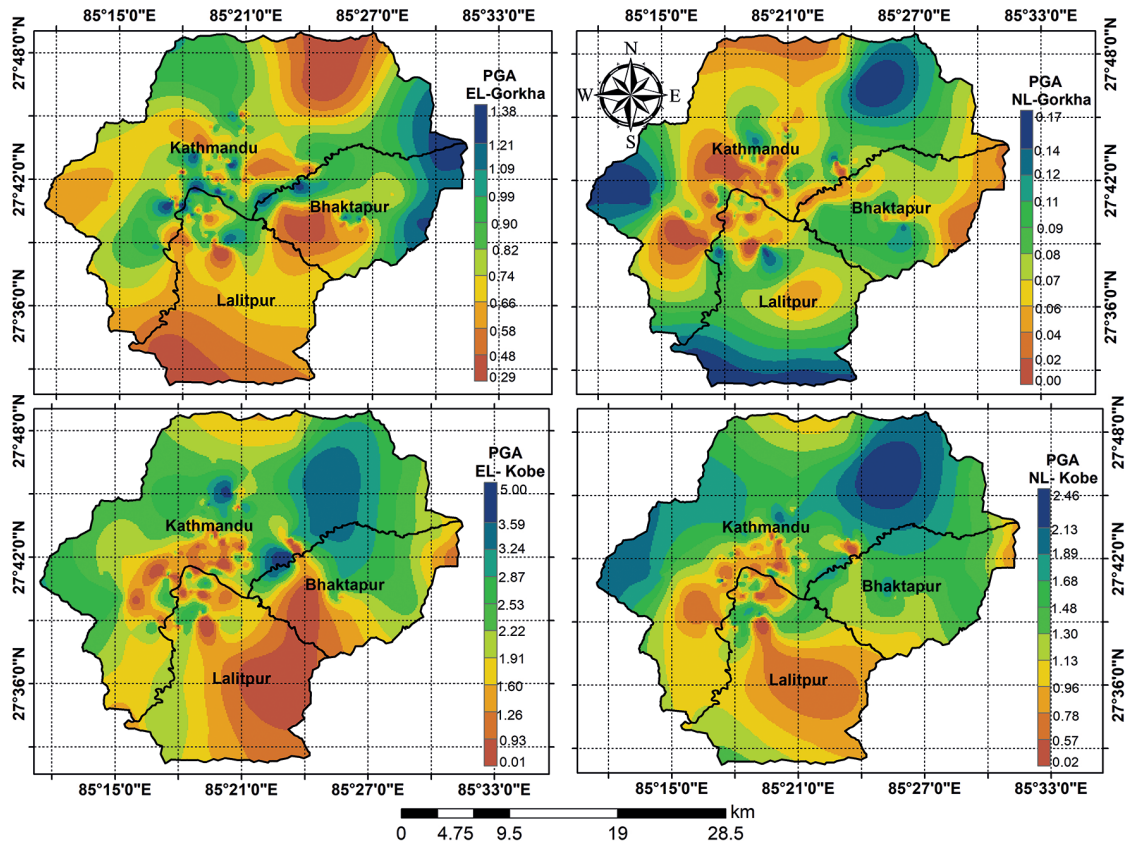
Fig. 7 - Spatial distribution of *PGA* in the Kathmandu Valley from DEEPSOIL™ simulations in EL and NL analyses for the 2015 Gorkha and 1995 Kobe earthquake motions.

4.2. Statistical comparison between PGA and displacement

Regression and statistical tests were performed between *PGA* (x-axis) and displacement (y-axis) to verify the observed *PGA* trends. Scatter plots with regression lines are shown in Fig. 8, and boxplots are presented in Fig. 9. The regression analysis yielded four sets of linear fit parameters, corresponding to different earthquake cases under EL and NL conditions. These parameters represent the slope and interception of the linear regression models fitted to the *PGA* against the displacement data. Here, *y* represents displacement and *x* represents *PGA* for both the EL and NL analysis. For the Gorkha EL case, the regression equation is given by $y = -0.197 \times x + 0.84$. The negative slope indicates a weak inverse correlation between *PGA* and displacement, suggesting that displacement slightly decreases as *PGA* increases. However, the magnitude of the slope is relatively small, implying that the relationship is not strongly pronounced. In the Kobe EL case, the regression fit is expressed as $y = 0.088 \times x + 0.27$. Here, the positive slope suggests a weak direct correlation, where an increase in *PGA* leads to a slight increase in displacement. Compared to the Gorkha EL case, the Kobe EL slope is smaller in magnitude, indicating a weaker effect.

The Gorkha NL case exhibits a substantially different trend, with the regression equation $y = -20.195 \times x + 0.979$. The significantly large negative slope implies a strong inverse relationship between *PGA* and displacement, indicating that under NL conditions, increasing *PGA* leads to

a substantial reduction in displacement. This behaviour is characteristic of NL soil behaviour, where higher ground motion intensities may trigger stiffness degradation and energy dissipation mechanisms, thereby limiting displacement. Finally, for the Kobe NL case, the regression equation is $y = -0.058 \times x + 0.263$. Although the slope is negative, its small magnitude suggests only a weak inverse correlation between *PGA* and displacement. Compared to the Gorkha NL case, the effect of *PGA* on displacement in the Kobe NL scenario is less significant. The results indicate that the NL cases exhibit stronger variations in displacement trends compared to their elastic counterparts. In particular, the Gorkha NL case shows a marked reduction in displacement with increasing *PGA*, likely due to soil nonlinearity and energy dissipation mechanisms. The Kobe NL case, while exhibiting a negative trend, shows a much smaller slope, indicating a weaker influence of nonlinearity. The elastic cases show relatively small slope values, reinforcing the observation that displacement remains more stable with increasing *PGA* when NL effects are not dominant. These findings highlight the importance of considering NL effects in ground motion analysis and infrastructure resilience assessments.

The scatter plots, as shown in Fig. 8, demonstrate how displacement varies with *PGA*; the fitted regression lines highlight the trends. In the Gorkha EL case, the correlation between *PGA* and displacement is weakly negative, with a statistically significant *p*-value of 0.0112 (Fig. 8a). Similarly, for the Kobe EL case, a weak positive trend is observed, with a *p*-value of 0.0211 (Fig. 8c), indicating statistical significance but weaker than that of the Gorkha EL case. The NL conditions show a different behaviour, particularly for the Gorkha NL case, where displacement decreases more significantly with *PGA*, reflected in a highly significant *p*-value of zero (Fig. 8b). In contrast, the Kobe NL case exhibits a weaker correlation, with a *p*-value of 0.0670 (Fig. 8d), suggesting that the NL effects do not strongly influence displacement.

The comparative boxplots shown in Fig. 9 provide insights into the differences between the two earthquake events under EL and NL conditions. The *PGA* EL comparison reveals that the Gorkha EL case has a higher median *PGA* than the Kobe EL case, with a *p*-value of 0.0112 confirming statistical significance. In the NL case, a significant contrast is observed between
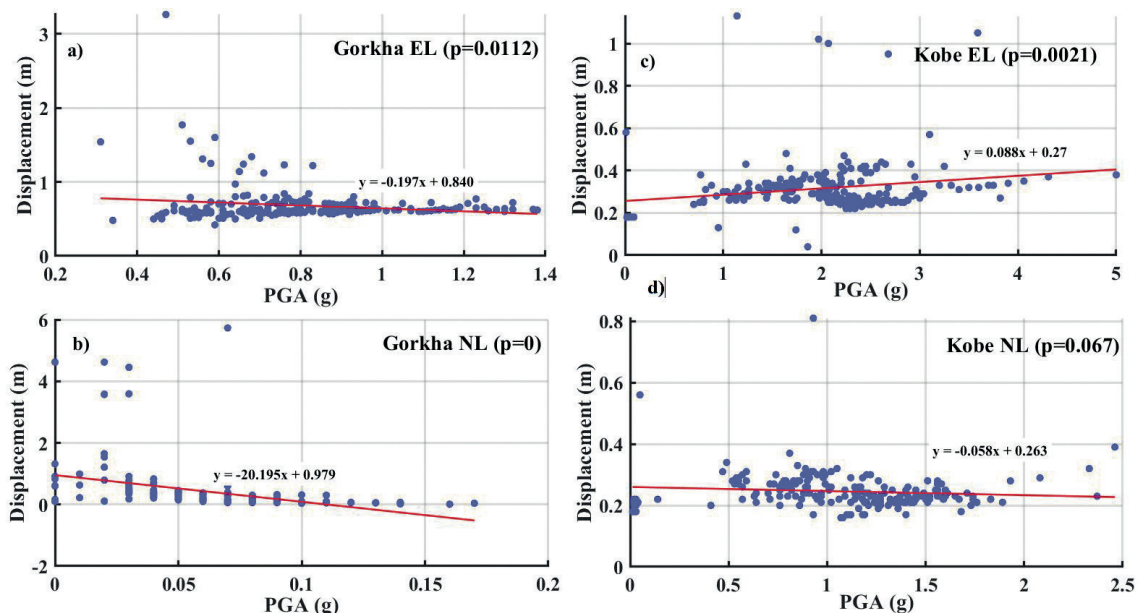

Fig. 8 - Comparison between *PGA* and displacement with *p*-value, where *y* is displacement and *x* is *PGA*.
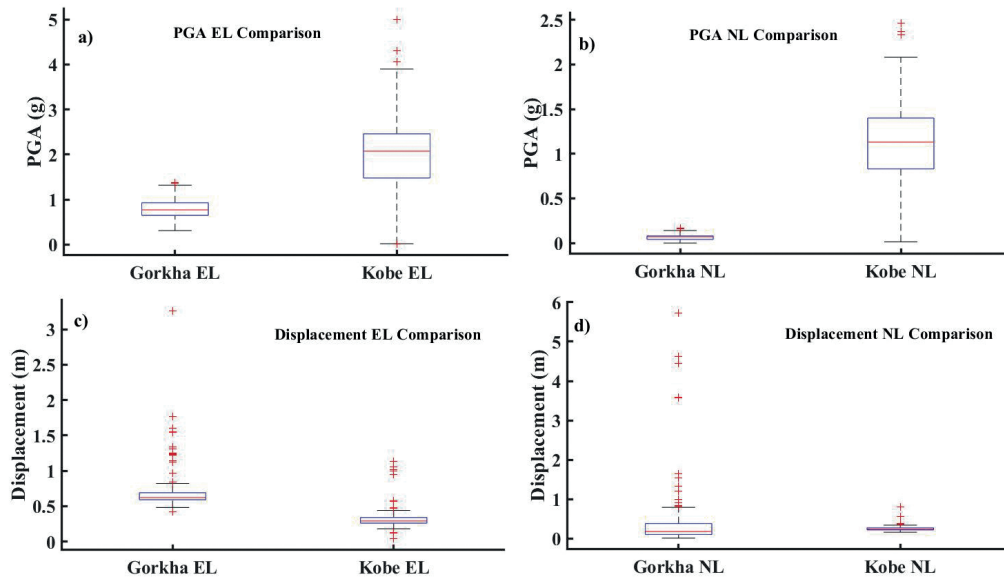
Fig. 9 - Comparative boxplots for *PGA* and displacement.

Gorkha and Kobe, with the *p*-value of zero highlighting a strong statistical difference. Regarding displacement, the Gorkha EL case shows slightly higher values than the Kobe EL case, with a *p*-value of 0.0211, while the NL comparison reveals a less pronounced difference, with a *p*-value of 0.0670. The presence of outliers, particularly in the Gorkha EL and Gorkha NL cases, suggests occasional extreme displacement values.

The findings indicate that elastic responses significantly influence displacement behaviour, especially in the Gorkha EL case, while NL effects play a crucial role in reducing displacement in the Gorkha NL case. The Kobe EL and NL cases exhibit weaker correlations, with their *p*-values indicating less statistical significance. The boxplots further confirm the substantial differences in *PGA* and displacement distributions between the two earthquakes, particularly under EL conditions. The inclusion of *p*-values provides a quantitative measure of statistical significance, reinforcing the observed trends in the scatter plots and highlighting the complex nature of the seismic response.

The noticeably higher *PGA* (NL) values observed in the Kobe NL case compared to the Gorkha NL (Fig. 8b) can be primarily attributed to local site conditions and instrumental recording differences. The Kobe Takatori station is situated in an area with relatively stiff soil or shallow bedrock, which may amplify high frequency seismic waves under strong-motion events. In contrast, the PTN station in the Kathmandu Valley is located in deep, soft sediment deposits that tend to attenuate high frequency motion and increase displacement but not necessarily *PGA*. Additionally, the Kobe earthquake had significantly higher input energy and near-source effects, which further contributed to higher *PGA* values.

This analysis underscores the importance of distinguishing between elastic and NL conditions when evaluating seismic displacement behaviour. The results of this study align with previous research indicating that NL soil behaviour plays a crucial role in modifying seismic response characteristics. Similar studies on NL ground response analysis have reported a reduction in displacement due to energy dissipation mechanisms, particularly in high intensity seismic events. The observed strong inverse correlation between *PGA* and displacement in the Gorkha NL case supports these findings, demonstrating that increased ground motion intensity leads to soil softening and increased damping effects.

However, the weaker NL influence observed in the Kobe NL case may be due to differences in earthquake characteristics or site specific soil properties. Previous studies have shown that variations in soil type, moisture content, and compaction levels can significantly influence the degree of nonlinearity in seismic response. The relatively higher *PGA* values in the Kobe event compared to the Gorkha may also contribute to the observed differences, as NL effects tend to be more pronounced in high-intensity shaking scenarios.

Xiao *et al.* (2022) conducted a study in China using DEEPSOIL™ and found that EL analysis overestimated seismic response in strong events, especially in soft soil sites, where NL analysis revealed a weakening effect. This study similarly shows that EL analysis overestimates *PGA* and displacement in clayey silt and silty sand regions, supporting the conclusion that NL analysis provides a more realistic representation of ground response in such soil conditions. Johari and Heidari (2020) analysed the Coyote Lake earthquake using QUAKE and observed that EL analysis underestimated *PGA* compared to NL analysis. In contrast, this study found an overestimation of *PGA* by EL analysis, suggesting that the impact of EL analysis may vary depending on soil type and seismic intensity. Additionally, the increased computational time required for NL analysis, was observed as noted in their study.

Mahmood *et al.* (2020) studied a site in Peshawar, Pakistan, and reported that both EL and NL methods produced similar soil amplification factors, but the EL method slightly overestimated *PGA*. This finding aligns with this, as the EL method consistently yielded higher values than the NL for *PGA*, although the magnitude of overestimation varied depending on soil type. Similarly, Tran *et al.* (2021) conducted research in Hanoi and found that EL analysis produced higher *PGA* values than NL analysis (0.2 g versus 0.16 g). Their study also suggested that local design codes might not fully capture site amplification effects. Likewise, this study demonstrates that EL analysis overestimates seismic response in the Kathmandu Valley, emphasising the necessity of considering NL effects in seismic hazard assessments.

Previous research has highlighted the susceptibility to liquefaction in various locations across the valley. Unlike prior major earthquakes, the impact of the Gorkha earthquake in triggering liquefaction seems to have been limited and concentrated. This could potentially be attributed to the moderate ground motion as well as lower groundwater levels. Specifically, Hattiban, Mulpani, and Duwakot were identified as areas where liquefaction occurred according to reports by Poudyal *et al.* (2024). Extensive liquefaction occurred at the Nepal Engineering College located on the left bank of the Monahara River. Sand boiling and fissures occurred, and the college buildings slightly subsided (Okamura *et al.*, 2015). Subedi and Acharya (2022) offer deeper insights into the liquefaction induced by the 2015 Gorkha earthquake. The low liquefaction occurrence in the valley is attributed to a low *PGA* of 0.17 g in the valley which is much smaller than the design *PGA* of 0.3 g in the studies of the liquefaction susceptibility maps (Sharma *et al.*, 2019). Furthermore, Gautam and Chamlagain (2016) highlighted notable local amplification and motion variations within soft soil deposits, particularly affecting areas like Thimi and Bhaktapur. Bhaktapur, especially since the 1255 earthquake, has faced severe damage, whereas Thimi consistently exhibits damage patterns similar to Bhaktapur.

These contrasting perspectives provide crucial insights into the complex soil seismic processes in the Kathmandu Valley. While the linear study offered a simplified overview, the NL analysis delved deeper, unravelling the intricate dynamics of soil behaviour. Hence, the choice between these approaches significantly influences the hazard assessments and earthquake resistant structures. Consequently, evaluating the strengths and limitations of each method becomes imperative for a comprehensive understanding of the intricate soil-seismic interactions prevalent in the Kathmandu Valley.

While this study provides valuable insights into the effects of nonlinearity on ground response, several limitations should be acknowledged. First, the analysis is based on a limited number of earthquake events, and additional case studies would be beneficial to validate the trends observed across different seismic conditions. Second, the regression models used in this study provide a linear approximation of the relationship between *PGA* and displacement; however, NL relationships may better capture using advanced statistical or machine learning approaches. The outcomes of this study were validated by comparing them with both field observations and previously published research. The observed trends, particularly the reduction in displacement under NL conditions, are consistent with findings by Mahmood *et al.* (2020), Tran *et al.* (2021), and Xiao *et al.* (2022), who similarly reported overestimation of PGA in EL analyses and damping effects in NL analyses. Additionally, the observed spatial patterns of displacement and liquefaction in the Kathmandu Valley, such as those near Mulpani, Hattiban, and Duwakot, support the modelled results, reinforcing the credibility of ground response predictions. These comparisons substantiate that DEEPSOIL™ based NL analysis provides a more realistic assessment of ground motion behaviour in soft sedimentary basins like the Kathmandu Valley.

Future research should explore the influence of soil type and stratigraphy on NL seismic response, as well as the impact of varying input motion characteristics. Incorporating 3D ground motion simulations and high resolution soil models could further enhance the accuracy of NL ground response predictions. Additionally, expanding the dataset to include more earthquake events from different tectonic settings would provide a more comprehensive understanding of NL seismic behaviour.

5. Conclusions

This study provides a comparative statistical analysis of EL and NL site response analyses for the Kathmandu Valley, focusing on their influence on *PGA* and displacement. Based on the results, the following key conclusions are drawn: NL soil behaviour significantly alters seismic response, especially under high intensity ground motions. The Gorkha NL case revealed a strong inverse relationship between *PGA* and displacement due to energy dissipation and soil softening.

EL models tend to overestimate *PGA* and displacement compared to NL models, particularly in soft soils like clayey silt and silty sand; this highlights the limitations of using EL methods in regions with highly NL soil behaviour. Statistical analysis confirms the significance of these trends, with the Gorkha NL case showing the strongest correlation ($p < 0.001$), underscoring the importance of considering nonlinearity in seismic design.

Validation against field data and previous studies supports the observed trends, indicating that DEEPSOIL™-based NL analysis provides a realistic approximation of ground response in sedimentary basins like the Kathmandu Valley.

Site specific NL analysis should be integrated into seismic hazard assessments to improve the accuracy of displacement predictions and to guide earthquake resistant design strategies in data-scarce and geologically complex regions.

The selection of appropriate input motions and statistical tools is critical for obtaining reliable predictions in ground response analysis.

Future research should expand on these findings by incorporating:
- a broader range of earthquake events;
- advanced NL modelling techniques;
- machine learning algorithms for pattern recognition;
- 3D ground motion simulations for improved site-specific hazard assessments.

REFERENCES

Amjadi A.H. and Johari A.; 2022: *Stochastic nonlinear ground response analysis considering existing boreholes locations by the geostatistical method*. Bull. Earthquake Eng., 20, 2285-2327, doi: 10.1007/s10518-022-01322-1.

Bhusal B., Aaqib M., Paudel S. and Parajuli H.R.; 2022: *Site specific seismic hazard analysis of monumental site Dharahara, Kathmandu, Nepal*. Geomatics, Nat. Hazards Risk, 13, 2674-2696, doi: 10.1080/19475705.2022.2130109.

Chamlagain D. and Gautam D.; 2015: *Seismic hazard in the Himalayan intermontane basins: an example from Kathmandu valley, Nepal.* In: Shaw R. and Nibanupudi H.K. (eds), Mountain Hazards and Disaster Risk Reduction, pp. 73-103, doi: 10.1007/978-4-431-55242-0_5.

Delaviz A., Yaghmaei-Sabegh S. and Souri O.; 2024**:** *Seismic fragility and reliability of base-isolated structures with regard to superstructure ductility and isolator displacement considering degrading behavior*. J. Earthquake Eng., 28, 3973-4002, doi: 10.1080/13632469.2024.2360120.

Dicleli M. and Buddaram S.; 2007: *Comprehensive evaluation of equivalent linear analysis method for seismic-isolated structures represented by sdof systems*. Eng. Struct., 29, 1653-1663, doi: 10.1016/j.engstruct.2006.09.013.

Edinçliler A. and Tuncay G.S.; 2018: *Nonlinear and equivalent linear site response analysis for the Bodrum region*. Eurasian J. Civ. Eng. Archit., 2, 59-68.

Falcone G. Boldini D. Martelli L. and Amorosi A.; 2020: *Quantifying local seismic amplification from regional charts and site specific numerical analyses: A case study*: Bull. Earthq. Eng., 18, 77–107, doi: 10.1007/s10518-019-00719-9.

Gautam D. and Chamlagain D.; 2016: *Preliminary assessment of seismic site effects in the fluvio-lacustrine sediments of Kathmandu valley, Nepal*. Nat. Hazards, 81, 1745-1769, doi: 10.1007/s11069-016-2154-y.

Gautam D., Chaulagain H., Rodrigues H. and Shahi H.R.; 2017: *Ground response based preliminary microzonation of Kathmandu valley*. Geotech. Eng., 48, 87-92.

Groholski D.R., Hashash Y.M.A., Kim B., Musgrove M., Harmon J. and Stewart J.P.; 2016: *Simplified model for small-strain nonlinearity and strength in 1D seismic site response analysis*. J. Geotech. Geoenviron. Eng., 142, 04016042, doi: 10.1061/(asce)gt.1943-5606.0001496.

Guragain S., Gautam S., Pokharel K., Shrestha A. and Lamichhane P.R.; 2020: *Soil amplification factor zonation of Kathmandu valley.* In: Proc. 8th IOE Graduate Conference, Pulchwok Campus, Lalitpur, Nepal, 8, pp. 761-767.

Hashash Y.M.A., Musgrove M.I., Harmon J.A., Ilhan O., Xing G., Numanoglu O., Groholski D.R., Phillips C.A. and Park D.; 2020: *Deepsoil 7.0 user manual*. Board of Trustees of University of Illinois at Urbana-Champaign. Urbana, Il, USA, 170 pp.

Iswanto E.R. and Yee E.; 2016: *Comparison of equivalent linear and non linear methods on ground response analysis: case study at west Bangka site*. J. Pengembangan Energi Nuklir, 18, 23, doi: 10.17146/jpen.2016.18.1.2994.

Johari A. and Heidari A.; 2020: *Comparison of equivalent linear and nonlinear ground response analysis methods in the time domain.* In: 3rd National & 1st International Conference on applied researches in Civil Engineering, Architecture and Urban Planning, Munich, Germany, 7 pp.

Khan S. and Waseem M.; 2019: *Earthquake seismic site response analysis by comparison between equivalent linear and nonlinear methods, a case study at Kohat and Muzaffarabad*. J. Himal. Earth Sci., 52, 46-63.

Kramer S.L.; 1996: *Geotechnical earthquake engineering.* Prentice Hall, Upper Saddle River, NJ, USA, 653 pp.

Mahmood K., Khan S.A., Iqbal Q., Karim F. and Iqbal S.; 2020: *Equivalent linear and nonlinear site-specific ground response analysis of Pashto Cultural Museum Peshawar, Pakistan*. Iran. J. Sci. Technol., Trans. Civ. Eng., 44, 179-191, doi: 10.1007/s40996-020-00346-4.

Mishra S., Sil A. and Das A.K.; 2025: *Site-specific ground response assessment of Bhubaneswar city, India, using 1D equivalent linear analysis: a case study*. Indian Geotech. J., 55, 3344-3371, doi: 10.1007/s40098-025-01187-6.

National Planning Commission; 2022: *Nepal Census 2021*. <censusnepal.cbs.gov.np/Home/Details?tpid=9>.

Okamura M., Bhandary N.P., Mori S., Marasini N. and Hazarika H.; 2015: *Report on a reconnaissance survey of damage in Kathmandu caused by the 2015 Gorkha Nepal earthquake*. Soils Found., 55, 1015-1029, doi: 10.1016/j.sandf.2015.09.005.

Pagliaroli A., Aprile V., Chamlagain D., Lanzo G. and Poovarodom N.; 2018: *Assessment of site effects in the Kathmandu valley, Nepal, during the 2015 Mw 7.8 Gorkha earthquake sequence using 1D and 2D numerical modelling*: Eng. Geol., 239, 50-62, doi: 10.1016/j.enggeo.2018.03.011.

Pandey B. and Jakka R.S.; 2022: *Selection of an appropriate bedrock for site amplification studies*: Nat. Hazards, 112, 216**7-2**195, doi: 10.1007/s11069-022-05260-8.

Poudyal D.; 2019: *Response analysis for multi layered soil*. J. Earthquake Sci. Soil Dyn. Eng., 2, 1-8.

Poudyal D., Roslan S.N.A. and Dahal B.K; 2022: *Seismic microzonation of Kathmandu valley: a review.* In: Proc. International Conference on Engineerig & Technology, IV, Kantipur Engineering College, Dhapakhel, Lalitpur, Nepal, pp. 85-89.

Poudyal D., Nordin N., Roslan S.N.A. and Dahal B.K.; 2024: *Spatial mapping of seismic vulnerability index in Kathmandu valley: insight from dominant frequency and amplification factor*. J. Geophys. Eng., 21, 1272-1285, doi: 10.1093/jge/gxae069.

Poudyal D., Nordin N. and Roslan S.N.A.; 2025a: *Comparative declustering approaches for seismic data: insights from Gardner- Knopoff, Gruenthal, Reasenberg, and Uhrhammer in the Kathmandu valley*. Ann. Geophys., 68, NH215, doi: 10.4401/ag-9178.

Poudyal D., Nordin N. and Roslan S.N.A.; 2025b: *Estimation and mapping of Arias intensity in Nepal: insights from seismic analysis in the Kathmandu valley*. Contrib. Geophys. Geod., 55, 31-47, doi: 10.31577/congeo.2025.55.1.3.

Poudyal D., Nordin N. and Roslan S.N.A.; 2025c: *Integrated earthquake risk assessment using PSHA-based microzonation and soil vulnerability index maps of urban Kathmandu valley*. Ann. Geophys., 68, S217, doi: 10.4401/ag-9246.

Saifuddin, Sungkono and Widodo A.; 2021: *S-wave velocity (Vs) model uncertainty derived from multiple equations of Vs and number of blows (N) at Institut Teknologi Sepuluh Nopember, Surabaya, Indonesia*. J. Phys. Conf. Ser., 1951, 012050, doi: 10.1088/1742-6596/1951/1/012050.

Sharma K., Deng L. and Khadka D.; 2019: *Reconnaissance of liquefaction case studies in 2015 Gorkha (Nepal) earthquake and assessment of liquefaction susceptibility*. Int. J. Geotech. Eng., 13, 326-338, doi: 10.1080/19386362.2017.1350338.

Subedi M. and Acharya I.P.; 2022: *Liquefaction hazard assessment and ground failure probability analysis in the Kathmandu valley of Nepal*. Geoenviron. Disasters, 9, doi: 10.1186/s40677-021-00203-0.

Tran N.L., Aaqib M., Nguyen B.P., Nguyen D.D., Tran V.L. and Nguyen V.Q.; 2021: *Evaluation of seismic site amplification using 1D site response analyses at Ba Dinh square area, Vietnam*. Adv. Civ. Eng., 2021, 3919281, doi: 10.1155/2021/3919281.

Wang J., Xie Y., Guo T. and Du Z.; 2023: *Predicting the Influence of soil-structure interaction on seismic responses of reinforced concrete frame buildings using convolutional neural network*. Buildings, 13, 564, doi: 10.3390/buildings13020564.

Xiao M., Cui J., Li Y.D. and Nguyen V.Q.; 2022: *Nonlinear seismic response based on different site types: soft soil and rock strata*. Adv. Civ. Eng., ID 5370369, 10, doi: 10.1155/2022/5370369.

Yildiz Ö.; 2021: *Nonlinear and equivalent linear site response analysis of Istanbul soils*: NATURENGS MTU J. Eng. Nat. Sci. Malatya Turgut Ozal Univ., 2, 88-101, doi: 10.46572/naturengs.895283.

Zhang X-ling., Fang L-jing., Xu C-shun., Jia K-min. and Han Y.; 2023: *Influence analysis of overlying soil layer to seismic behavior of inclined liquefiable soil and pile interaction system*. Soil Dyn. Earthquake Eng., 169, 107876, doi: 10.1016/j.soildyn.2023.107876.

Corresponding author: Dibyashree Poudyal
                            Department of Civil Engineering, Infrastructure University Kuala Lumpur (IUKL)
                            43000 Kajang, Selangor Darul Ehsan, Malaysia
                            Phone +9779840090607; e-mails: 082101900007@s.iukl.edu.my, dibyashreel@nec.edu.np